

# Structural and Electrochemical Analysis of $\text{SmBa}_{0.8}\text{Sr}_{0.2}\text{Co}_2\text{O}_{5+\delta}$ Cathode Oxide for IT-SOFCs

Adi Subardi<sup>1\*</sup>, Ade Indra<sup>2</sup>, Jan Setiawan<sup>3</sup>, Yen-Pei Fu<sup>4</sup>

<sup>1</sup>Department of Mechanical Engineering,  
Institut Teknologi Nasional Yogyakarta (ITNY), DIY 55281, INDONESIA

<sup>2</sup>Department of Mechanical Engineering,  
Institut Teknologi Padang, West Sumatera 25173, INDONESIA

<sup>3</sup>National Nuclear Energy Agency of Indonesia,  
Kawasan PUSPIPTEK, Banten 15310, INDONESIA

<sup>4</sup>Department of Materials Science and Engineering,  
NDHU, Hualien 97401, TAIWAN

\*Corresponding Author

DOI: <https://doi.org/10.30880/ijie.2023.15.01.015>

Received 17 August 2021; Accepted 28 October 2021; Available online 28 February 2023

**Abstract:** The double perovskite  $\text{SmBa}_{0.8}\text{Sr}_{0.2}\text{Co}_2\text{O}_{5+\delta}$  (SBSC82) was prepared using a conventional technique and evaluated as solid oxide fuel cells (SOFCs) cathode material which operates at intermediate temperatures. The SBSC82 cathode powder was produced using the solid-state reaction technique and an alumina ball as a grinder. XRD was used to determine the cathode powder structure, and the microstructure was analyzed using SEM. The oxygen content ( $\delta$ ) for the SBSC82 cathode was recorded by a thermogravimetric analyzer. Powder patterns and lattice parameters were detected using General Structure Analysis System (GSAS) software. The symmetrical cell was examined using a Voltalab PGZ 301 potentiostat. The  $\delta$  of SBSC82 cathode reached 5.68, 5.43, and 5.22 at 400°C, 600°C, and 800°C. It was found that SBSC82 oxide show as a simple perovskite-type structure with tetragonal P4/mmm. The polarization resistance ( $R_p$ ) of the symmetrical cell with SDC|SBSC82|SDC configuration reached of 0.420  $\Omega\cdot\text{cm}^2$ , 0.091  $\Omega\cdot\text{cm}^2$ , and 0.041  $\Omega\cdot\text{cm}^2$  at 650°C, 750°C, and 850°C, respectively. Single cell specimen achieves a power density of 377  $\text{mW}/\text{cm}^2$  under humidified air/hydrogen.

**Keywords:** SOFC, SBSC82, crystal structure, electrochemical, cell performance

## 1. Introduction

Electrical energy is an essential resource for humans, both for commercial and industrial applications as well as for domestic activities. Traditional fossil energy sources are becoming increasingly limited, and a growing disparity exists between increased demand and electricity production from renewable energy sources. Fulfilling energy demand requires the development of new technologies, especially power plants, for the survival of society and the global economy. Renewable energy has various advantages, including varied fuel sources and low pollution, which has attracted the interest of researchers in the last few decades in developing fuel cells. SOFC achieves the highest efficiency and greater fuel flexibility than other fuel cell groups.

Work [1] reported that reduced operating temperatures could benefit from sealing and thermal depreciation, facilitating using less expensive metal connection materials and reducing interactions involving cell components, all of which can assist in reducing IT-SOFC costs. The cathode is a limiting factor in deciding the efficiency of the overall

SOFC. Therefore, the design of novel electrodes for the oxygen reduction reaction with a high electrocatalytic response is very relevant for IT-SOFCs. The authors [2] revealed the cathode material requirements for SOFC applications: 1. The thermal expansion coefficient corresponding to other cell components, 2. Oxygen reduction reactions (ORR) require high catalytic activity, 3. At high temperatures, electrolytes and interconnects show chemical stability, and 4. Electrical conductivity is acceptable ( $>100$  S/cm). Due to their excellent electrochemical performance, double perovskites have become interesting structures for application in IT-SOFCs operating at  $600^{\circ}\text{C}$ - $800^{\circ}\text{C}$ .

Generally, the double perovskites where the rare earth (RE) ions occupy site A, the barium occupies site A, and site B occupies cobalt. Substitution of Sr for Ba in membrane  $\text{LnBaCo}_2\text{O}_{5+\delta}$  perovskite can increase electrical conductivity and enhance cathode electrochemical behavior. Meanwhile, the Co element can decrease polarization activation during oxygen reduction activation [3]. The oxygen binding strength is reduced and disorder-free pathways for ionic motion are provided by converting a membrane crystal with alternating lanthanide and alkali earth planes from a simple cubic perovskite with randomly occupied A-sites. As a result, the oxygen diffusivity should theoretically increase. The  $\text{Sr}^{2+}$  substitution effect of  $\text{Ba}^{2+}$  in  $\text{LnBaCo}_2\text{O}_{5+\delta}$  provides the following advantages: (1) high electrical conductivity, (2) increased oxygen content, (3) excellent resistance polarization ( $R_p$ ) value, and (4) good chemical stability [4]. With superior characteristics such as high void oxygen concentration, high electronic conductivity, and good catalytic activity, double perovskite materials have received increased attention. It has been intensively researched, the characteristics of the double layer perovskite cathode material with the chemical formula  $\text{LnBaCo}_2\text{O}_{5+\delta}$  (Ln-selected lanthanide) [5]. A lot of works using various lanthanides and alkaline earth metals into the A-site of double perovskites to enhance oxygen mobility in the LnO field include  $\text{LaBa}_{0.5}\text{Sr}_{0.25}\text{Ca}_{0.25}\text{Co}_2\text{O}_{5+\delta}$  [6]  $\text{LnBa}_{0.5}\text{Sr}_{0.5}\text{Co}_{1.5}\text{Fe}_{0.5}\text{O}_{5+\delta}$  (Ln=La and Nd) [7],  $\text{SmBa}_{0.5}\text{Sr}_{0.5}\text{Co}_2\text{O}_{5+\delta}$  [8],  $\text{PrBa}_{0.5}\text{Sr}_{0.5}\text{Co}_{2-x}\text{Fe}_x\text{O}_{5+\delta}$  [9],  $\text{PrBa}_{0.5}\text{Sr}_{0.5}\text{Co}_{2-x}\text{Ni}_x\text{O}_{5+\delta}$  [10],  $\text{YBa}_{1-x}\text{Sr}_x\text{Co}_2\text{O}_{5+\delta}$  [11],  $\text{GdBa}_{1-x}\text{Sr}_x\text{Co}_2\text{O}_{5+\delta}$  ( $0 \leq x \leq 1.0$ ) [12],  $\text{LaBa}_{0.5}\text{Sr}_{0.5}\text{Co}_2\text{O}_{5+\delta}$  [13]. Thus, it is a relevant task to investigate the crystal structure, oxygen content ( $\delta$ ), electrochemical and cell performances, and the microstructure of SBSC82 as a cathode material at medium temperature.

## 2. Experimental

### 2.1 Preparation of the Anode, Electrolyte, and Cathode Materials

The electrolyte and electrode material were prepared following a procedure previously published [14]. The sol-gel process was used to prepare the SDC ( $\text{Sm}_{0.2}\text{Ce}_{0.8}\text{O}_{1.9}$ ) electrolyte material using precursors consisting of  $\text{Sm}(\text{NO}_3)_3 \cdot 6\text{H}_2\text{O}$  (99%) and  $\text{Ce}(\text{NO}_3)_3 \cdot 6\text{H}_2\text{O}$  (99%) The cathode material composition consisting of  $\text{Sm}_2\text{O}_3$  (99%),  $\text{BaCO}_3$  (98.8%),  $\text{SrCO}_3$  (98%), and  $\text{CoO}$  (99.9%) was calculated by the stoichiometry method. The anode preparation process includes drying, powder refinement, and granulation with polyvinyl alcohol (PVA) using 60 mesh. Alumina balls in liquid alcohol were used to grind the cathode material for 12 hours and then dried at  $65^{\circ}\text{C}$ . Next stage, the cathode material was calcined at  $1100^{\circ}\text{C}$  and maintained for 4 hours, then was cooled to room temperature. In the next step, the cathode material was smoothed using a mortar pestle and filtered with a 200mesh screen. The NiO,  $\text{Sm}_2\text{O}_3$ , and carbon were combined in liquid alcohol as the anode material. A hydraulic press machine was used for making the half-cell and single-cell specimens.

Screen-printing techniques to fabricate the symmetrical cell (half-cell) design SBSC82|SDC|SBSC82. Each side of the electrolyte disk surface was coated with cathode slurry (paste). Next step, the cathode slurry was applied to the electrolyte surface and then sintered at a temperature of  $1000^{\circ}\text{C}$ . The cathode paste was screened on one face as a working electrode, with a total area of  $0.385\text{ cm}^2$ . The Ag electrode reference and the working electrode were separated by about 0.4 cm. On the opposite side of the SDC disk, the Cathode Counter Electrode (CE) was implanted [15]. Specimen testing included X-ray diffraction (XRD) measurements and electrochemical, microstructure, and single-cell (voltage-current) studies to determine the power density of the cathode. The thickness and diameter of single cell specimens were 13 mm and 1 mm with SDC|SDC|SBSC82 configuration. Please refer to our previous publications [16] for detailed procedures to fabricate single cells.

### 2.2 Specimen Testing

An XRD (Rigaku D/MAX-2500V) with a scanning range of  $20^{\circ}$  to  $80^{\circ}$  was used to characterize the SBSC82 cathode structure. The JADE 5 program was used to compare the sample crystal structure to the XRD pattern provided by the XRD database. All the XRD patterns (including the background) are refined during the refinement process using various parameters such as space groups, atomic positions, atomic site placement, and atomic thermal parameters. Rietveld's refinement analyzed the powder pattern and lattice parameters using the GSAS program. The Rietveld refinement uses a model structure and initial crystal structure parameters taken from previous references, including structural parameters reported in the literature, which are adopted as initial values. The SBSC82 cathode surface microstructure and a half-cell cross-section were identified by SEM (Hitachi 3500H). The symmetrical cell specimens were tested in the air at  $50^{\circ}\text{C}$  intervals between  $600^{\circ}\text{C}$  and  $800^{\circ}\text{C}$ . The AC impedance observations were made using a VoltaLab PGZ301 potentiometer, and the amplitude of the AC signal was set to 10 mV at a frequency ranging from

100 kHz-0.1 Hz. The data for electrochemical impedance spectroscopy was analyzed using the Z-view application [3], and a digital source meter was conducted to collect the single cell data.

### 3. Results and Discussion

#### 3.1 The Structure of SBSC82 Cathode

The GSAS program was used to analyze the diffraction patterns of calcined SBSC82 specimens at 1100°C, as presented in Figure 1 (a). The crystallographic information of the SBSC82 cathode is presented in Table 1. The Rietveld refinement data for SBSC82 was identified as tetragonal (P4/mmm), and the lattice parameters are shown in Table 2. The practical information and the measured profiles are remarkably consistent, demonstrating that cation ions in a perovskite lattice are well-ordered between  $\text{Sm}^{3+}$  and  $\text{Ba}^{2+}/\text{Sr}^{2+}$  ions [17].

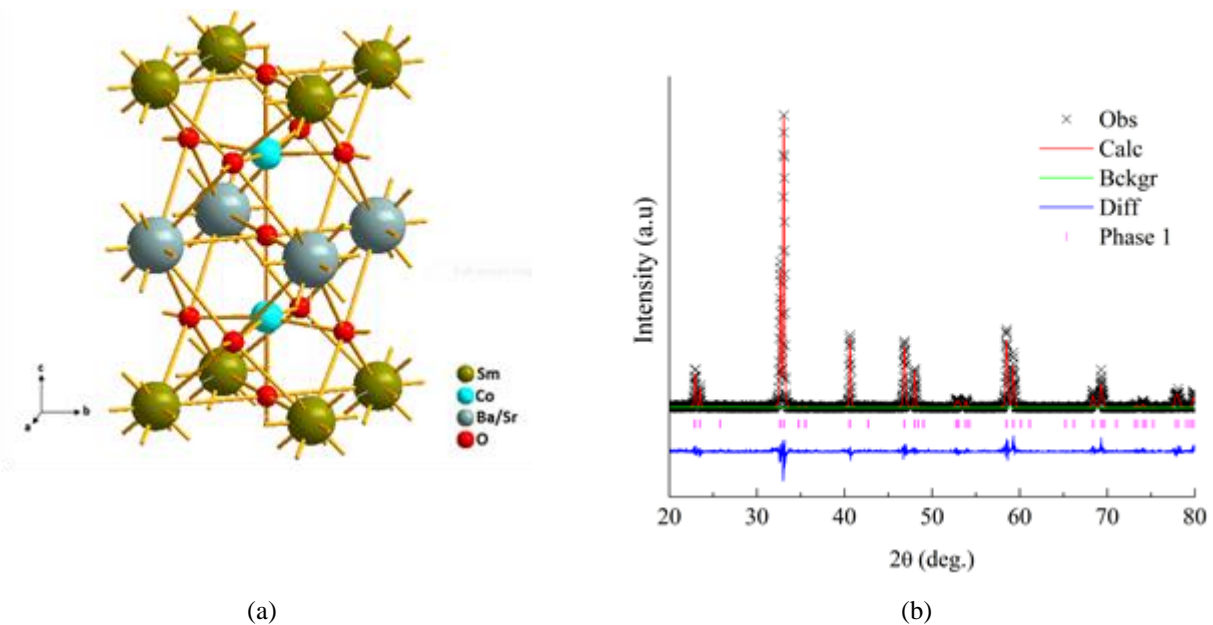


**Fig. 1 - (a) Crystal structure of the SBSC82 cathode at room temperature; (b) calculated (solid line) X-ray diffraction profiles, observed (crosses), and the difference (bottom line) of SBSC82 calcined at 1100°C**

**Table 1 - The crystallographic information of SBSC82 was collected through the Rietveld refining process**

Atom	Position of Wyckoff	X	Y	Z	Uiso
Samarium	1a(0 0 0)	0	0	0	0.012
Cobalt	2h(0.5 0.5 z)	0.5	0.5	0.246	0.002
Barium	1b(0 0 0.5)	0	0	0.5	0.015
O1	4i(0 0.5 z)	0	0.5	0.222	0.065
O2	1c(0.5 0.5 0)	0.5	0.5	0	0.004
O3	2h(0.5 0.5 z)	0.5	0.5	0.499	0.193
Strontium	1b(0 0 0.5)	0	0	0.5	0.044

In the crystal structure of the SBSC82 cathode, the Sm atoms are placed at 1a. Meanwhile, at 1b, the Ba and Sr atoms are dispersed randomly. Position 2h is occupied by the Co atom (0.5, 0.5, z), and three types of oxygen-atom locations can be found: O1 at the 4i (0,0.5, z) site, O2 at the 1c (0.5,0.5,0) site, and O3 at the 2h (0.5,0.5, z) site. An image of the SBSC82 cathode crystal structure at room temperature is shown in Figure 1 (b).

**Table 2 - The lattice characteristics of several cathode materials with a double-perovskite structure**

Samples	SG	a (Å)	b (Å)	c (Å)	V (Å)
LBSC55 [4]	Tetragonal	3.868	3.868	7.731	115.69
SBSC64 [5]	Tetragonal	3.870	3.870	7.590	114.11
SBSC55 [8]	Tetragonal	3.883	3.883	7.580	114.30
SBSC82 [this work]	Tetragonal	3.881	3.881	7.581	114.23

### 3.2 Oxygen Content ( $\delta$ )

The  $\delta$  of the SBSC82 cathode was determined using experimental data from the TGA (SII TG/DTA 6300). Figure 2 shows the  $\delta$  formed on the SBSC82 cathode oxide from 26°C to 1000°C. The  $\delta$  curve observed in the area between points A and D illustrate the behavior of the SBSC82 cathode oxide. The decrease in oxygen content between regions A to B is 0.09, and a significant decrease in oxygen content is recorded at 0.01 along point B (95°C) to point C (215°C).

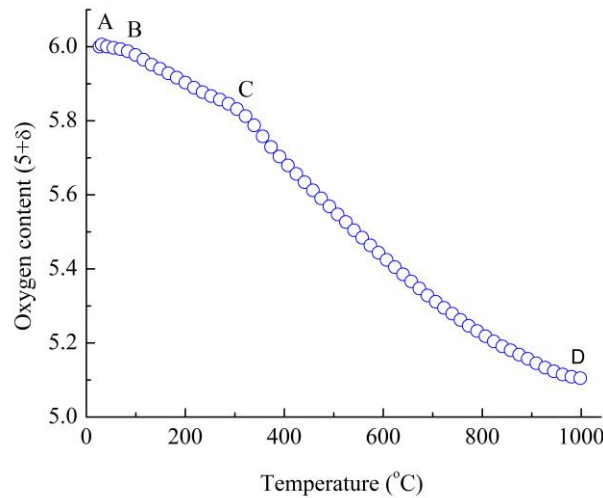


Fig. 2 - The  $\delta$  vs. temperature for sintered SBSC82 cathode specimen

Table 3 - The  $\delta$  for SBSC82 cathodes versus temperature in air

Samples	$(\delta)$			
	200°C	400°C	600°C	800°C
SBSC91 [3]	5.53	5.44	5.32	5.18
SBSC73 [3]	5.62	5.50	5.36	5.22
SBSC55 [3]	5.74	5.64	5.51	5.39
SBSC82 [this work]	5.90	5.68	5.43	5.22

From point C (306°C) to point D (1000°C), the  $\delta$  decrease was more significant, with oxygen reduction recorded at 0.9. The  $\delta$  versus temperature for SBSC82 cathode powder is presented in Fig. 2. The high  $\delta$  may lead to the enhanced surface activity of the oxygen reduction reaction (ORR) and higher oxide ion diffusivity in bulk [18]. The detailed  $\delta$  versus temperature is listed in Table 3.

### 3.3 Exchange Current Density ( $i_0$ )

The electrochemical behavior of the SBSC82 cathode was recorded by the impedance spectra based on the symmetrical cell of SBSC82|SDC|SBSC82 sintered at a temperature of 1000°C for four h. Fig. 3 shows the typical impedance spectrum obtained from the SBSC82 cathode using SDC as the electrolyte under open-circuit conditions. The polarization resistance ( $R_p$ ) values were collected at 0.420, 0.091, and 0.041  $\Omega \cdot \text{cm}^2$  at 650°C, 750°C, and 850°C, respectively. The  $R_p$  values, particularly at 750 and 850°C, meet the requirements for cathode resistance ( $<0.15 \Omega \cdot \text{cm}^2$ ) [19], and the  $R_p$  value achieved by the SBSC82 cathode-based single cell is lower than other cathodes such as PBSCN-1 (0.64  $\Omega \cdot \text{cm}^2$  at 750°C), PBSCN-2 (0.65  $\Omega \cdot \text{cm}^2$  at 750°C), PBSCN-3 (0.66  $\Omega \cdot \text{cm}^2$  at 750°C) [10], and LaBaCuFeO<sub>5+ $\delta$</sub>  (0.11  $\Omega \cdot \text{cm}^2$  at 750°C) [20].

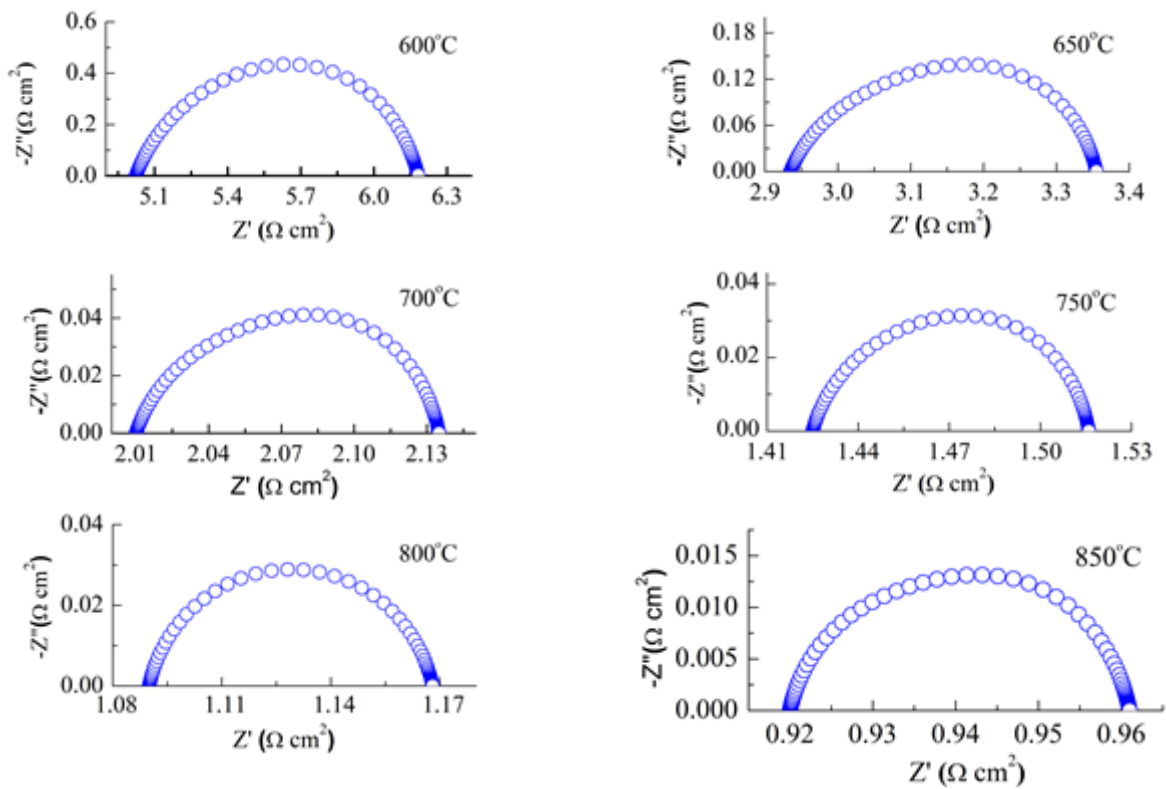


**Fig. 3 - Total polarization resistance ( $R_p$ ) of the SBSC82 cathode within the temperature range of 600°C-850°C**

In Table 4, the current density ( $i_o$ ) value generally increases with temperature increases. The  $i_o$  value significantly increased from 2.92 mA cm<sup>-2</sup> at 600°C to 25.42 mA cm<sup>-2</sup> at 850°C, which EIS determined. These findings show that SBSC82 oxide is a suitable cathode material for IT-SOFC.

**Table 4 - The current density ( $i_o$ ) values of SBSC82 cathode determined by the EIS method**

Temperature (°C)	Current density ( $i_o$ ) (mA.cm <sup>-2</sup> )
600	2.92
650	5.73
700	9.24
750	14.64
800	19.35
850	25.42

### 3.4 Single-Cell Performance

The Ni-SDC|SDC|SBSC82 single cell performance was tested in an air/humidified hydrogen (3 vol% H<sub>2</sub>O). The power density can achieve 377 mW/cm<sup>2</sup> at 650°C, as shown in Figure 4. For comparison, a single cell containing a cathode of lanthanum strontium manganite produced a power density of 13.06 mW/cm<sup>2</sup> at 700°C [21]. Generally, an ideal cell's open-circuit voltage (OCV) must be similar to the theoretical value of 1.1 V, and the operating conditions slightly affect it. In this work, the OCV levels tend to be lower than the theoretical levels, which may be due to several factors, such as (1) the Ce<sup>4+</sup> species in the SDC electrolyte is quickly decreased to Ce<sup>3+</sup>, particularly at higher temperatures. SDC electrolyte with low electronic conductivity causes a small flow of electrons (leakage current) through the electrolyte, and (2) oxidizing agents can pass through the electrolyte layer due to some porosity causing cell leakage current resulting in a low OCV value [3].

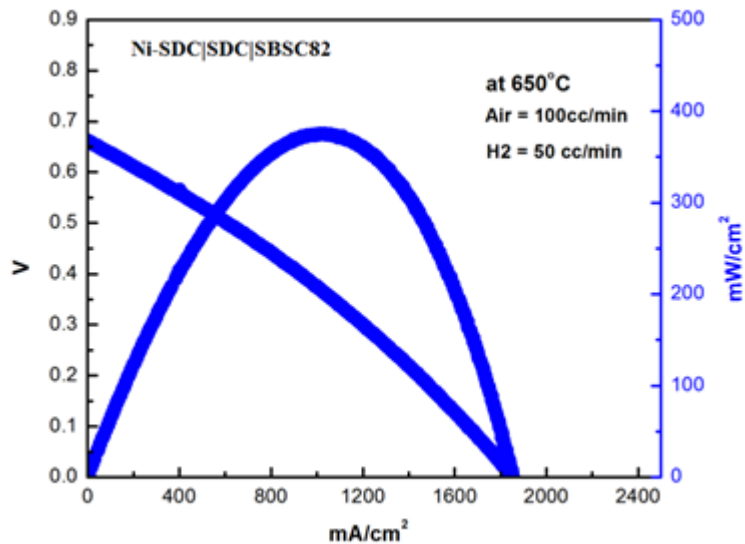


Fig. 4 - I - V curve of a single-cell specimen of Ni-SDC|SDC|SBSC82

### 3.5 SEM Image

Electron and oxygen transports are strongly related to the cathode structure, influencing fuel cell performance, including the reaction kinetics and the charge-transportation and mass-transportation preprocess. The half-cell microstructure of SBSC82|SDC|SBSC82 and a view of the cathode surface are presented in Figure 5, which shows that the cathode adhesion to the electrolyte is very strong. The grain size is spread evenly within the range of 1.5-2.5  $\mu\text{m}$ , and the structure is porosity. The good morphology of SOFC cells includes (1) a porous cathode microstructure, (2) strong interface connections (electrolyte-cathode), and (3) a dense electrolyte layer. A better morphology helps to ensure rapid oxygen diffusion, minimizes polarization resistance, and improves current collection.

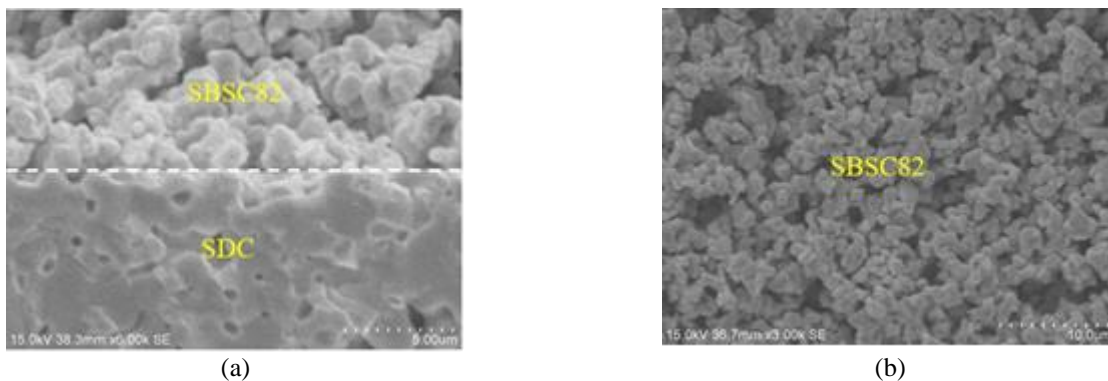


Fig. 5 - SEM (a) cross-sectional of the half cell and; (b) upper of the SBSC82 cathode

### 4. Conclusion

This study investigates the structural characteristics, oxygen content, electrochemical properties, and microstructure of SBSC82 cathodes. A GSAS analysis reveals that the SBSC82 cathode is based on the space group P4/mmm and tetragonal structure. The polarization resistance ( $R_p$ ) value obtained from EIS is 0.420, 0.091, and 0.041  $\Omega\cdot\text{cm}^2$  at 650°C, 750°C, and 850°C, respectively. The current-potential properties of single cell suggest that the power density was 377  $\text{mW}/\text{cm}^2$  at 650°C. All of the findings showed that the SBSC82 could be applied as effective electrode material in IT-SOFCs to produce electricity.

### Acknowledgments

The authors gratefully acknowledge the Ministry of Science and Technology for their support in performing this project with code MOST 106-2113-M-259-011. The authors are also grateful to Prof. Dr. Yen-Pei Fu, Taiwan.

## References

- [1] Subardi, A., Susanto, I., Kartikasari, R., Tugino, T., Kuntara, H., Wijaya, A.E., Purnomo, M.J., Indra, A., Fahmi, F., Fu, Y.P. (2021). An Analysis of  $\text{SmBa}_{0.5}\text{Sr}_{0.5}\text{Co}_2\text{O}_{5+\delta}$  Double Perovskite Oxide for Intermediate-Temperature Solid Oxide Fuel Cells. *Eastern-European Journal of Enterprise Technologies*, 2, 1-14.
- [2] Mohsen, F.V., Bahman, A.H. (2021). Progress in Material Development for Low-Temperature Solid Oxide Fuel Cells: A Review. *Energies*, 14, 1280-1335.
- [3] Subardi, A., Chen, C.C., Cheng, M.H., Chang, W.K., Fu, Y.P. (2016). Electrical, thermal and electrochemical properties of  $\text{SmBa}_{1-x}\text{Sr}_x\text{Co}_2\text{O}_{5+\delta}$  cathode materials for intermediate-temperature solid oxide fuel cells. *Electrochim Acta*, 204, 118-127.
- [4] Zhang, K., Ge, L., Ran R., Shao, Z., Liu, S. (2008). Synthesis, characterization and evaluation of cation-ordered  $\text{LnBaCo}_2\text{O}_{5+\delta}$  as materials of oxygen permeation membranes and cathodes of SOFCs. *Acta materialia*, 56, 4876-4889.
- [5] Garces, D., Mohni, L.V. (2020). High temperature transport properties of  $\text{La}_{0.5-x}\text{Pr}_x\text{Ba}_{0.5}\text{CoO}_{3-\delta}$  perovskite ( $x = 0, 0.2, 0.5$ ). *Solid State Ionics*, 347, 115239.
- [6] Yao C., Zhang, H., Liu, X., Meng, J., Zhang, X., Meng, F., Men, J. (2018). Characterization of layered double perovskite  $\text{LaBa}_{0.5}\text{Sr}_{0.25}\text{Ca}_{0.25}\text{Co}_2\text{O}_{5+\delta}$  as cathode material for intermediate-temperature solid oxide fuel cells. *Journal of Solid State Chemistry*, 265, 72-78.
- [7] Yang, Q., Tian, D., Liu, R., Wu, H., Chen, Y., Ding, Y., Lu, X., Li, B. (2021). Exploiting rare-earth-abundant layered perovskite cathodes of  $\text{LnBa}_{0.5}\text{Sr}_{0.5}\text{Co}_{1.5}\text{Fe}_{0.5}\text{O}_{5+\delta}$  ( $\text{Ln}=\text{La}$  and  $\text{Nd}$ ) for SOFCs. *Int. J. Hydrogen Energy*, 46, 5630-5641.
- [8] Lin, T.N., Lee, R.Y., Kuo, J.Y., Ishihara, T., and Hosoi, K. (2015). Fabrication of  $\text{SmBa}_{0.5}\text{Sr}_{0.5}\text{Co}_2\text{O}_{5+\delta}$  Cathode Material and Its Application for Sr- and Mg-Doped  $\text{LaGaO}_3$  Electrolyte-Supported Solid Oxide Fuel Cell. *ECS Trans.*, 68, 895-901.
- [9] Choi, S., Yoo, S., Kim, J., Park, S., Jun, A., Sengodan, S., Kim, J., Shin, J., Jeong, H.Y., Choi, Y., Kim, G., Liu, M. (2013). Highly efficient and robust cathode materials for low-temperature solid oxide fuel cells:  $\text{PrBa}_{0.5}\text{Sr}_{0.5}\text{Co}_{2-x}\text{Fe}_x\text{O}_{5+\delta}$ . *Sci. Rep.*, 3, 1-6.
- [10] Liu, L., Guo, Wang, S., Yang, Y., Yin, D. (2014). Synthesis and characterization of  $\text{PrBa}_{0.5}\text{Sr}_{0.5}\text{Co}_{2-x}\text{Ni}_x\text{O}_{5+\delta}$  ( $x=0.1, 0.2$  and  $0.3$ ) cathodes for intermediate temperature SOFCs. *Ceram. Int.*, 40, 16393-16398.
- [11] McKinlay, A., Connor, P., Irvine, J.T.S., Zhou, W.Z. (2007). Structural chemistry and conductivity of solid solution  $\text{YBa}_{1-x}\text{Sr}_x\text{Co}_2\text{O}_{5+\delta}$ . *J Phys Chem C*, 111, 19120-19125.
- [12] Kim, J.H., Prado, F., Manthiram, A. (2008). Characterization of  $\text{GdBa}_{1-x}\text{Sr}_x\text{Co}_2\text{O}_{5+\delta}$  ( $0 \leq x \leq 1.0$ ) double perovskites as cathodes for solid oxide fuel cells. *J Electrochem Soc.*, 155, B1023-B1028.
- [13] Subardi, A., Liao, K.Y., Fu, Y.P. (2017). Oxygen permeation, thermal expansion behavior and electrochemical properties of  $\text{LaBa}_{0.5}\text{Sr}_{0.5}\text{Co}_2\text{O}_{5+\delta}$  cathode for SOFCs. *RSC Adv.*, 7, 14487-14495.
- [14] Subardi, A., Cheng, M.H., Fu, Y.P. (2014). Chemical bulk diffusion and electrochemical properties of  $\text{SmBa}_{0.6}\text{Sr}_{0.4}\text{Co}_2\text{O}_{5+\delta}$  cathode for intermediate solid oxide fuel cells. *Int J Hydr Energy*, 9, 20783-20790.
- [15] Subardi, A., Fu, Y.P. (2018). Crystal structure, thermal expansion, and long-term behaviors of  $\text{SmBaCoO}_{5+\delta}$  as cathode for intermediate-temperature solid oxide fuel cells. *MATEC Web of Conferences*, 215, 01026.
- [16] Fu, Y.P., Ouyang, J., Li, C.H., S. Hu, S.H. (2013). Chemical bulk diffusion coefficient of  $\text{Sm}_{0.5}\text{Sr}_{0.5}\text{CoO}_{3-\delta}$  cathode for solid oxide fuel cells. *J Power Sources*, 240, 168-177.
- [17] Jun, A., Shin, J., Kim, G. (2013). High redox and performance stability of layered  $\text{SmBa}_{1-x}\text{Sr}_x\text{Co}_{1.5}\text{Cu}_{0.25}\text{O}_{5+\delta}$  perovskite cathodes for intermediate-temperature solid oxide fuel cells. *Phys Chem Phys.*, 15, 19906-19912.
- [18] Kim, A., Wang, S., Jacobson, A.J., Reimus, L., Brodersen, P., Mims, C.A. (2007). Rapid oxygen ion diffusion and surface exchange kinetics in  $\text{PrBaCo}_2\text{O}_{5+\delta}$  with a perovskite related structure and ordered a cation, *J. Mater. Chem.*, 17, 2500-2505.
- [19] Steele, B.C.H. (1996). Survey of materials selection for ceramic fuel cells II. Cathodes and anodes. *Solid State Ionics*, 86, 1223-1234.
- [20] Zhou, Q., He, T., He, Q., Ji Y. (2009). Electrochemical performances of  $\text{LaBaCuFeO}_{5+\delta}$  and  $\text{LaBaCuCoO}_{5+\delta}$  as potential cathode materials for intermediate-temperature solid oxide fuel cells. *Electrochemistry Communications*, 11, 80-83.
- [21] Gan, L., Zhong, Q., Song, Y, Li, L., Zhao, X. (2015).  $\text{La}_{0.7}\text{Sr}_{0.3}\text{Mn}_{0.8}\text{Mg}_{0.2}\text{O}_{3-\delta}$  perovskite-type oxides for NO decomposition by the use of intermediate temperature solid oxide fuel cells. *J Alloys Compd.*, 628, 390-395.